



UNIVERSITY  
OF WOLLONGONG  
AUSTRALIA

University of Wollongong  
Research Online

---

Faculty of Engineering - Papers (Archive)

Faculty of Engineering and Information Sciences

---

1999

# Fission converter and metal–oxide–semiconductor field effect transistor study of thermal neutron flux distribution in an epithermal neutron therapy beam

G. I. Kaplan

*University of Wollongong*

Anatoly B. Rosenfeld

*University of Wollongong, [anatoly@uow.edu.au](mailto:anatoly@uow.edu.au)*

B. J. Allen

*University of Wollongong*

J. A. Coderre

*Brookhaven National Laboratory, New York, USA*

H. B. Liu

*University of California, USA*

<http://ro.uow.edu.au/engpapers/150>

---

## Publication Details

This article was originally published as Kaplan, GI, Rosenfeld, AB, Allen, BJ et al, Fission converter and metal–oxide–semiconductor field effect transistor study of thermal neutron flux distribution in an epithermal neutron therapy beam, *Medical Physics*, 26(9), September 1999, 1989. Copyright American Association of Physicists in Medicine. Original journal available [here](#).

Research Online is the open access institutional repository for the University of Wollongong. For further information contact the UOW Library: [research-pubs@uow.edu.au](mailto:research-pubs@uow.edu.au)

# Fission converter and metal-oxide-semiconductor field effect transistor study of thermal neutron flux distribution in an epithermal neutron therapy beam

Greg I. Kaplan<sup>a)</sup>

*Department of Engineering Physics, University of Wollongong, Wollongong, 2522, Australia;  
Westmead Institute for Cancer Research, University of Sydney at Westmead Hospital, 2145, Australia*

Anatoly B. Rosenfeld

*Department of Engineering Physics, University of Wollongong, Wollongong, 2522, Australia*

Barry J. Allen

*St. George Cancer Care Centre, Kogarah, Australia; Department of Engineering Physics,  
University of Wollongong, Wollongong, 2522, Australia*

Jeffrey A. Coderre

*Brookhaven National Laboratory, Upton, New York*

Hungyan B. Liu

*Department of Neurological Surgery, University of California-Davis, Sacramento, California*

(Received 20 August 1998; accepted for publication 18 June 1999)

The depth distribution of the thermal neutron flux is a major factor in boron neutron capture therapy (BNCT) in determining the efficiency of cell sterilization. In this paper the fission detector method is developed and applied to measure the in-phantom thermal neutron flux depth distribution. Advantages of the fission detector include small size, direct measurement of thermal neutron flux in a mixed radiation field of BNCT beam, self-calibration, and the possibility of on-line measurement. The measurements were performed at epithermal a BNCT facility. The experimental results were compared with the thermal neutron flux calculated by the Monte Carlo method and found to be in good agreement. © 1999 American Association of Physicists in Medicine. [S0094-2405(99)01609-0]

Key words: BNCT, thermal neutrons, dosimetry, fission detector, MOSFET

## I. INTRODUCTION

In binary radiation therapy, cancer cells are selectively loaded with a nontoxic agent which is activated by a subsequent irradiation. In boron neutron capture therapy (BNCT),  $^{10}\text{B}$  atoms are selectively delivered to the cancer cells as a boronated compound and then the tumor zone is irradiated by neutrons. Tumor control in BNCT results from an exposure of cancer cells to the products of  $^{10}\text{B}(n, \alpha)^7\text{Li}$  reaction. Boron-10 captures a thermal neutron and decays releasing an alpha particle and a  $^7\text{Li}$  ion. Both reaction products have a short range, high linear energy transfer (LET) and are efficient in sterilizing a biological cell. The cross-section of this reaction,  $\sigma$ , depends strongly on the neutron energy. The cross-section has a maximum value for the thermal neutrons and decreases as  $\propto E^{-1/2}$  with the increasing neutron energy.<sup>1</sup> For achieving the best sterilization, a tumor must be exposed to thermal neutrons. The problem is that thermal neutrons have a low penetration ability in tissue (half value layer is less than 2 cm, dependent on field size). To deliver a significant fluence of thermal neutrons to a deeper tumor the irradiation has to be performed with an epithermal neutron beam. Epithermal neutrons moderate in tissue producing thermal neutrons at depth. Clinical trials of epithermal BNCT are being conducted at the Brookhaven Medical Research Reactor (BMRR), Brookhaven National Laboratory

(BNL) in New York,<sup>2</sup> MIT reactor in Cambridge, Massachusetts,<sup>3</sup> and have recently commenced at High Flux Reactor in Petten, the Netherlands.<sup>4</sup> In Japan, thermal neutrons are used to irradiate the tumor bed in intraoperative BNCT of brain tumors.<sup>5</sup>

As  $^{10}\text{B}$  is activated by thermal neutrons, the therapeutic effect of the BNCT is partly determined by the thermal neutron flux at the target depth. This makes experimental measurement of thermal neutron flux distribution at depth in a phantom important for dose planning and validation of Monte Carlo calculations. Measurement of the thermal neutron flux in a mixed neutron-gamma field is a complicated and time consuming task. The neutron flux at a BNCT facility is often measured by the foil activation cadmium difference method.<sup>6,7</sup> Two separate irradiations and postirradiation gamma activity measurements are required. The cadmium difference method utilizes cadmium as an absorber of thermal neutrons. Another method of thermal neutron flux measurement employs a  $^{10}\text{B}$  or  $^6\text{Li}$  coated ionization chamber. This method is not an absolute one as it requires calibration in a known radiation field.<sup>8,9</sup> The use of a  $^{235}\text{U}$  converter and a silicon diode in a current mode for beam monitoring was recently suggested but, to our knowledge, not yet implemented.<sup>10</sup> This method is also not an absolute one.

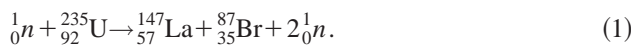
A fission detector provides an alternative method of ther-

mal neutron flux measurement which has been used in nuclear reactor applications.<sup>11</sup> A fission detector is an absolute radiation detector for measurement of neutron fluence, requiring a single irradiation without postirradiation measurement of neutron induced activity, and does not require a calibration in a known radiation field. It also offers a possibility of on-line monitoring of thermal neutron flux. In the present paper we report the development and application of a specially designed fission detector for the direct in-phantom measurement of thermal neutron flux distribution in an epithermal BNCT beam. Another aim of this report was to develop and test metal-oxide-semiconductor field effect transistor (MOSFET) semiconductor detectors for in-phantom measurement of thermal neutron flux and boron response at BNCT facilities.

## II. MATERIALS AND METHODS

### A. Fission detector

The main part of the fission detector used in this study was a 150- $\mu\text{m}$ -thick uranium (99.25%  $^{235}\text{U}$  enrichment) converter. The converter was deposited on an aluminum foil and was placed in contact on the surface of a small size ( $3 \times 3 \text{ mm}^2$ ) ion implanted silicon detector.  $^{235}\text{U}$  has a large thermal neutron capture cross-section,  $\sigma = 580$  barns for 2200 m/s neutrons.<sup>12</sup> When  $^{235}\text{U}$  captures a thermal neutron, it fissions with a probability of  $p = 85\%$ <sup>13</sup> into one of about 40 modes. A typical nuclear reaction is:



Two heavy fragments move in opposite directions and carry a total kinetic energy of 162 MeV.<sup>13</sup> In a pulse height spectrum the high energy fragments are well separated from the low LET gamma background and recoil protons produced by neutron interactions with the phantom material. This separation makes the fission detector efficient for thermal neutron measurements in a mixed radiation field. The fast neutrons which are released in the  $^{235}\text{U}$  fission reaction have a low cross-section of interaction with  $^{235}\text{U}$  and for this reason are not captured by  $^{235}\text{U}$  and do not trigger a further fission reaction in the converter.

Alpha particles released in a spontaneous decay of  $^{235}\text{U}$  at an energy of 4.5 MeV were used as an internal energy standard for energy calibration of the detector. The range of these alpha particles in uranium, as calculated by TRIM,<sup>14</sup> is  $R_\alpha = 7.37 \mu\text{m}$ . Only an alpha particle originating within the layer of thickness  $R_\alpha$ , adjacent to the detector has a chance to enter the detector and to be registered. The volume of this layer is  $R_\alpha \times A$ , where  $A$  is the surface area of the converter. The total number of  $^{235}\text{U}$  atoms in the  $R_\alpha$  thick layer is  $N_U = n_U \times R_\alpha \times A$ , where  $n_U$  is the volume concentration of  $^{235}\text{U}$  atoms in the converter. If a spontaneous alpha decay of a uranium atom occurs at the depth  $x$  under the surface of the converter ( $x \leq R_\alpha$ ), the alpha particle reaches the detector only if it is projected within the cone of solid angle  $\Omega$  (Fig. 1).

We assume that the angular distribution of alpha particles is uniform. The fraction of alpha particles, which is regis-

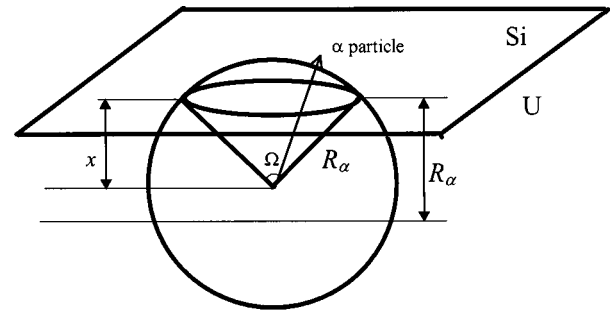


Fig. 1. Sketch of the geometry of a decay particle production in the uranium converter of the fission detector (below the horizontal plane) and particle entering the silicon detector (above the plane).

tered after being emitted from the depth  $x$  (Fig. 1), equals the ratio of part of the surface area of sphere of the radius  $R_\alpha$  above the converter surface to the total surface area of the sphere

$$\frac{2\pi \times R_\alpha(R_\alpha - x)}{4\pi \times R_\alpha^2} = \frac{R_\alpha - x}{2R_\alpha}.$$

If the number of disintegrations per second within the layer  $R_\alpha$  is  $A_t$  then the detector registers  $N_\alpha$  alpha particles per second, i.e.

$$N_\alpha = \frac{A_t}{R_\alpha} \int_0^{R_\alpha} \frac{R_\alpha - x}{2R_\alpha} dx = \frac{A_t}{4}, \text{ or } A_t = 4N_\alpha. \quad (2)$$

The number of uranium atoms in  $R_\alpha$  thick layer of the uranium converter can be calculated as

$$N_U = \frac{A_t \times \tau}{\ln 2}, \text{ or } n_U = \frac{4N_\alpha \times \tau}{R_\alpha \times A \times \ln 2}, \quad (3)$$

where  $\tau$  is the half life of  $^{235}\text{U}$ ,  $\tau = 7.1 \times 10^8 \text{ yr}$ .<sup>13</sup>

For calculating the response of the fission detector we assume that in a radiation field of thermalized neutrons the angular distribution of  $^{235}\text{U}$  fission fragments is close to uniform. For simplicity we also assume that all of the fission reactions proceed in single mode [Eq. (1)] and  $^{147}\text{La}$  and  $^{87}\text{Br}$  nuclei are released. Kinetic energy of each fragment separately can be calculated by applying conservation of kinetic energy and linear momentum laws;  $E_{\text{La}} = 60 \text{ MeV}$  and  $E_{\text{Br}} = 102 \text{ MeV}$ . Ranges of the fragments, as calculated by TRIM, equal  $R_{\text{La}} = 4.35 \mu\text{m}$  and  $R_{\text{Br}} = 6.23 \mu\text{m}$ . Note:  $R_\alpha > R_{\text{Br}} > R_{\text{La}}$ . Only  $^{147}\text{La}$  nuclei produced within  $R_{\text{La}}$  layer and  $^{87}\text{Br}$  nuclei produced within  $R_{\text{Br}}$  layer can reach the detector. As for the above alpha particle consideration [Fig. 1 and Eq. (2)], only one quarter of the fragments produced within the corresponding layers will be registered. Number of  $^{147}\text{La}$  nuclei,  $N_{\text{La}}$  registered by the detector per second equals

$$N_{\text{La}} = \frac{1}{4} \Phi \times p \times \sigma \times n_U \times R_{\text{La}} \times A,$$

where  $\Phi$  is the thermal neutron flux. Similarly the number of  $^{87}\text{Br}$  nuclei,  $N_{\text{Br}}$ , registered by the detector per second equals

$$N_{\text{Br}} = \frac{1}{4} \Phi \times p \times \sigma \times n_U \times R_{\text{Br}} \times A.$$

Because both of the fragments have a spherically uniform distribution of the velocities, the total flux of fission products registered by the detector equals  $N_f = N_{La} + N_{Br}$ . Substituting  $n_U$  from Eq. (3), the thermal neutron flux equals

$$\Phi = \frac{N_f \times R_\alpha \times \ln 2}{p \times \sigma \times N_\alpha \times \tau \times (R_{La} + R_{Br})}. \quad (4)$$

A pair of identical  $3 \times 3 \text{ mm}^2$  Si detectors were used with and without the fission converter, each with an energy resolution of 15 keV. The same size silicon detector with 1%  $^{10}\text{B}$  converter was applied for the relative measurement of boron response.

### B. MOSFET detector

The method of paired MOSFET detectors was applied<sup>15</sup> for measurement of boron dose enhancement. A MOSFET detector was operated in active mode at gate bias voltage of +5 V. Under this condition the sensitivity of the detector to 6 MV LINAC x-ray was about 5 mV per cGy. One of the two MOSFETs was covered with 1%  $^{10}\text{B}$  converter while the other was not. The radiation dose was measured at the same depth in a phantom by both detectors and the boron dose was obtained by subtraction of the response after normalizing the reading of the bare MOSFET to the  $^{10}\text{B}$  covered one.

### C. Phantoms and Monte Carlo calculation

Dosimetric and spectral measurements were performed in a  $15 \times 15 \times 15 \text{ cm}^3$  perspex cube phantom. Radiation detectors were placed at different depths from the surface along the central axis of the perspex phantom.

A Monte Carlo transport code for neutron and photon transport (MCNP, version 4a) was applied for computation of the thermal neutron flux along the central axis of the perspex cube phantom.<sup>16</sup> This calculation simulated tracks of individual neutrons and photons from an experimentally validated source plane at the irradiation port of the BMRR epithermal neutron irradiation facility, generated three-dimensional thermal neutron flux distribution in the phantom.

### D. Neutron therapy irradiation facility

BMRR<sup>17</sup> is a light-water moderated and cooled and graphite reflected research reactor with operating power up to 3 MW. It became operational in 1959 and has both thermal and epithermal neutron irradiation facilities. At the epithermal neutron irradiation facility,<sup>18</sup> current clinical trials are being performed by irradiating patients with the epithermal neutron beam operated at the full power. The very high count rate and consequent high dead time of a silicon detector, make it impossible to conduct spectroscopy measurements at full reactor power. Consequently, reactor power of 20 kW was used for silicon detectors, assuming linearity of beam intensity as a function of reactor power. MOSFET measurements were performed at the full reactor power.

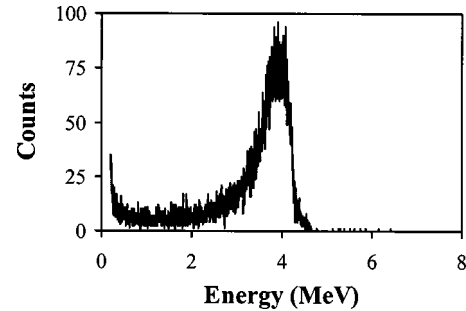


Fig. 2. Spectrum of spontaneous alpha decay of  $^{235}\text{U}$  in the fission converter.

### III. RESULTS AND DISCUSSION

$^{235}\text{U}$  spontaneously decays by releasing an alpha particle with an energy of 4.5 MeV. The energy spectrum of alpha particles in the absence of an external radiation field (Fig. 2) was used for energy calibration of the fission detector and for verifying the calibration during the experimental measurements at the irradiation facilities. Because alpha particle emission originates from different depths in the converter, the alpha particle peak is broadened and shifted to lower energies. The maximum energy corresponds to 4.5 MeV, while the main peak is observed at an energy of  $\sim 3.9$  MeV. The alpha particle count rate was measured to be  $N_\alpha = 2.26$  counts per second.

The pulse height spectrum of the epithermal neutron beam incident on the perspex phantom was measured by the silicon detector without the  $^{235}\text{U}$  converter (Fig. 3) at a depth of 1.3 cm, and does not show any counts for deposited energies above 1 MeV. The spectrum in Fig. 3 is typical for all the phantom depths used in the experiments. Since the fission fragments have much greater energies and LET than recoil protons and gamma rays, the fragment pulse height spectrum does not overlap with the spectrum of low energy or low LET radiation present in the radiation field.

Measurements with a fission detector were performed at the depths of 1.3, 3.7, 6.2, and 11 cm in the perspex phantom. A pulse height spectrum of the fission detector exposed to epithermal neutrons exhibits a broad double peak of fission fragments in the energy range up to 90 MeV (Fig. 4). When the thermal neutron flux decreases with an increase in phantom depth, this double peak becomes lower in intensity

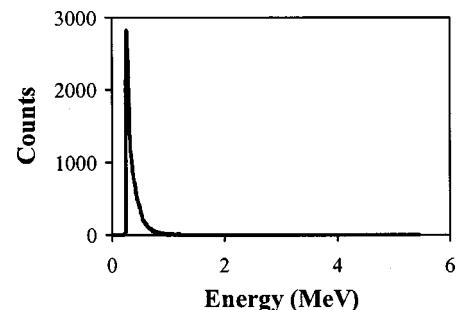


Fig. 3. Gamma and recoil proton spectrum at the epithermal neutron irradiation facility at BMMR, reactor power 20 kW.

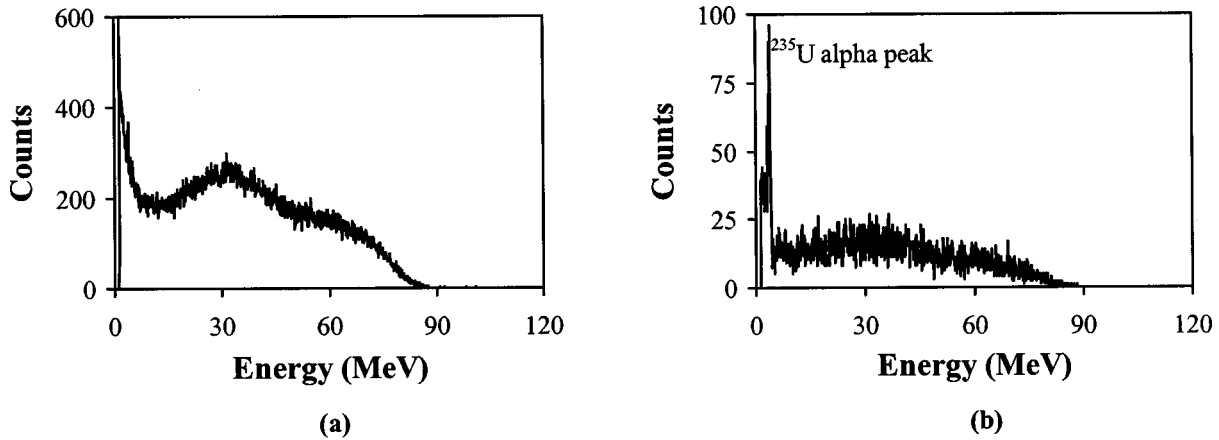


FIG. 4. Uranium fission fragment spectra at 1.3 cm (a) and 11 cm (b) depth in perspex phantom. (Epithermal neutron irradiation facility at BMRR, reactor power 20 kW.)

and the alpha particle peak, originating from the spontaneous alpha decay of uranium, becomes more apparent [Fig. 4(b)].

The area under the broad double peak of fission fragments was measured and normalized to the time of measurement. Equation (4) was applied to calculate the thermal neutron flux at each depth of measurement. Equation (4) depends on the ratio of ranges of alpha particle and fission fragments, and its ratio is not sensitive to the exact composition of the converter. The ratio equals 0.70 for U and 0.69 for  $UO_2$ . A numerical factor of 150 was applied for conversion of the thermal neutron flux measured at 20 kW to that at 3 MW reactor power. The experimental error of measurements was estimated as 7%.

The thermal neutron flux in the perspex phantom was calculated by MCNP along the phantom central axis with steps of 0.5 cm. An energy of 0.4 eV was used in the Monte Carlo calculation as a separator between thermal and intermediate neutrons. The statistical error estimate of all the calculated data was below 1%.

The experimental data, scaled to 3 MW reactor power, are compared with the Monte Carlo calculation in Fig. 5(a). The agreement is good, the experimental points being located within the error limits from the Monte Carlo calculated curve. Energy dependence of  $^{235}U$  neutron capture cross-section is similar to that of  $^{10}B$ , or  $\sigma \propto E^{-1/2}$ , for neutron energies of up to 1 eV. Above this energy significant resonance structure is observed<sup>19</sup> which increases the cross section from the  $\propto E^{-1/2}$  dependence, and introduces a systematic error to the fission detector measurements at higher neutron energies. However, the thermalization of the neutrons in a phantom and large thermal neutron fission cross section reduces the impact of this systematic error which does not exceed the total uncertainty of measurements.

Relative data on boron response were obtained by comparison of measurements by  $^{10}B$  covered silicon detector with the measurements by a bare silicon detector at the same points in the phantom. The relative boron response was in very good agreement with the thermal neutron fluxes mea-

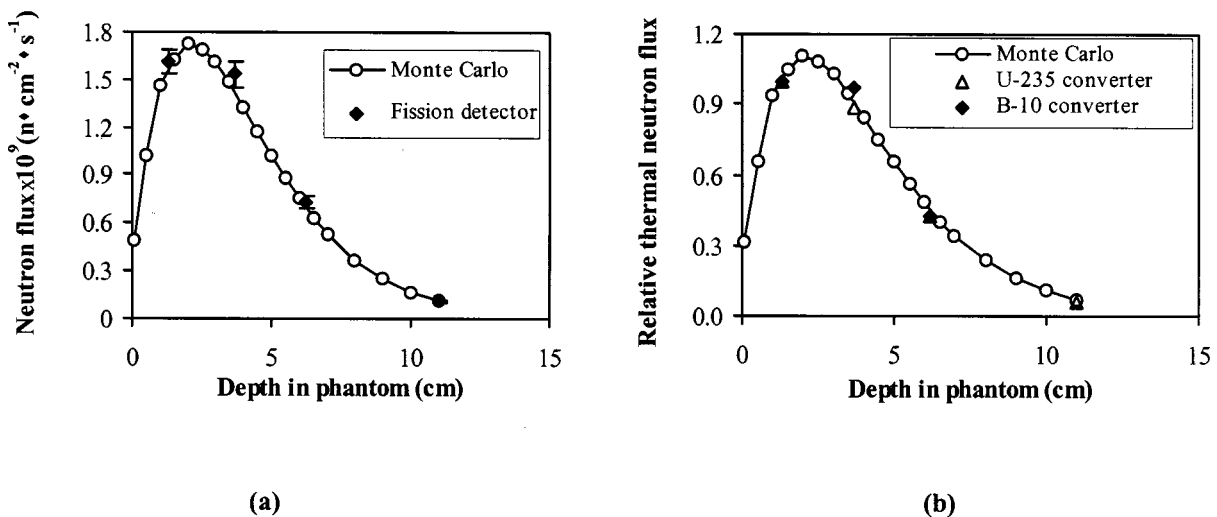


FIG. 5. Thermal neutron flux along the central axis of the perspex phantom irradiated at BMRR. (a) Monte Carlo calculation and measurement by Si detector with  $^{235}U$  converter. (b) Relative thermal neutron flux and relative response of detectors with  $^{235}U$  and  $^{10}B$  converters.



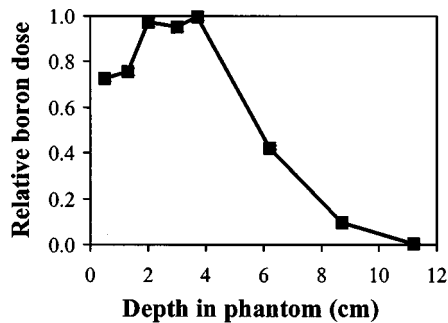


FIG. 6. Relative in phantom, boron dose depth distribution for the BMRR epithermal beam.

sured by the uranium fission detector and calculated by the Monte Carlo code [Fig. 5(b)]. This agreement shows that boron capture and uranium fission have the same response to the incident epithermal neutron beam.

The paired MOSFET detector method<sup>15</sup> was used with the BMRR beam for dosimetry of depth distribution of the relative boron dose. MOSFET response was measured at 3 MW reactor power along the central axis of the perspex phantom. The dose was measured at each depth in the phantom by a bare MOSFET sensor and by an identical MOSFET coated by a boron-containing plastic. Readings of the bare MOSFET were subtracted from the readings of the boron coated MOSFET. The difference between the readings is ascribed to the boron dose enhancement. Results were normalized to the maximum measured dose and are plotted in Fig. 6. In the mixed epithermal neutron-gamma radiation field, the maximum boron dose enhancement occurs at the depths of 2–4 cm from surface. This is in agreement with the maximum in the depth distribution of thermal neutron flux (see Fig. 5).

#### IV. CONCLUSION

The <sup>235</sup>U converter fission detector was developed and successfully applied for in-phantom measurements of thermal neutron flux distribution for an incident epithermal BNCT. The agreement between fission detector measured and Monte Carlo calculated fluxes was good. Advantages of the uranium converter fission detector are an internal on-line calibration by alpha particles from spontaneous uranium decay; fast measurement which requires a single reactor run; small size of the detector which minimizes radiation field perturbation (i.e., smaller than a miniature ionization chamber), and the possibility of on-line monitoring of the thermal neutron flux.

A thinner converter should be used, preferably with the thickness of about 1  $\mu\text{m}$ , to improve the accuracy of a fission detector. A smaller size silicon detector will also reduce further the perturbation of the radiation field and increase the dose-depth resolution of the detector.

The paired MOSFET detectors, with and without boron cover, was found to successfully measure the relative thermal neutron flux, showing good agreement with the fission detector and Monte Carlo calculations.

#### ACKNOWLEDGMENTS

We would like to thank Professor P. G. Litovchenko from Kiev Institute for Nuclear Research for providing us with the <sup>235</sup>U converter. We are grateful to Detector Ltd, Ukraine for the manufacturing of the silicon detectors used in this study. We further appreciate the support of the dedicated staff at BMRR.

<sup>a</sup>)Electronic mail: gkaplan@uow.edu.au

<sup>1</sup>J. R. Lamarsh, *Introduction to Nuclear Reactor Theory* (Addison-Westley, Reading, MA, 1966).

<sup>2</sup>M. Chadha, J. Capala, J. A. Coderre, E. H. Elowitz, J. Iwai, D. D. Joel, H. B. Liu, L. Wieloploski, and A. D. Chanana, "Boron neutron capture therapy (BNCT) for glioblastoma multiform (GBM) using the epithermal neutron beam at the Brookhaven National Laboratory," *Int. J. Radiat. Oncol., Biol., Phys.* **40**, 829–834 (1998).

<sup>3</sup>P. M. Busse, R. Zamenhoff, H. Madoc-Jones, G. Solares, S. Kiger, K. Riley, C. Chuang, G. Rogers, and O. Harling, "Clinical Follow-up of Patients with Melanoma of the Extremity Treated in a Phase I Boron Neutron Capture Therapy Protocol," in *Advances in Neutron Capture Therapy*, edited by B. Larsson, J. Crawford, and R. Weinreich (Elsevier, Lausanne, 1997), Vol. 1, pp. 60–64.

<sup>4</sup>W. Sauerwein, "The Clinical Project at HFR Petten—a Status Report," in *Advances in Neutron Capture Therapy*, edited by B. Larsson, J. Crawford, and R. Weinreich (Elsevier, Lausanne, 1997), Vol. 1, pp. 77–82.

<sup>5</sup>Y. Hayakawa, S. Harasawa, A. Nakamoto, K. Amano, H. Hatanaka, and J. Egawa, "Simultaneous monitoring system of thermal neutron flux for boron neutron capture therapy," *Radiat. Res.* **75**, 243–251 (1978).

<sup>6</sup>S. K. Sofar, J. Kalef-Ezra, R. G. Faichild, B. H. Laster, S. Fiarman, and E. Ramsay, "Epithermal Beam Development at BMRR: Dosimetric Evaluation," in *Neutron Beam Design, Development and Performance for NCT*, edited by O. Harling *et al.* (Plenum, New York 1990), pp. 307–316.

<sup>7</sup>C. P. J. Raaijmakers, M. W. Konijnenberg, H. W. Verhagen, and B. J. Mijnheer, "Determination of dose components in phantom irradiated with an epithermal neutron beam for boron neutron capture therapy," *Med. Phys.* **22**, 321–329 (1995).

<sup>8</sup>R. Schmidt, R. L. Maughan, M. Yudelev, C. Kota, and S. Wanwilairat, "Experimental determination of the thermal neutron flux around two different types of high intensity <sup>252</sup>Cf sources," *Med. Phys.* **26**, 83–86 (1999).

<sup>9</sup>G. Solares, D. Katz, O. Harling, and R. Zamenhof, "On-Line Dosimetry for Boron Neutron Capture Therapy at the MIT Research Reactor," in *Advances in Neutron Capture Therapy*, edited by B. Larsson, J. Crawford, and R. Weinreich (Elsevier, Lausanne, 1997), Vol. 1, pp. 147–152.

<sup>10</sup>Y. Hayakawa, Y. Nakagawa, and H. Hatanaka, "Simultaneous Monitoring System of Neutron Fluence Rate Distribution by Detectors with Multiple Sensitive Heads" in *Cancer Neutron Capture Therapy*, edited by Mishima (Plenum, New York, 1996), pp. 473–477.

<sup>11</sup>J. M. McKenzie and D. A. Bromley, "Observation of charged particle reactor products," *Phys. Rev. Lett.* **2**, 303–305 (1959).

<sup>12</sup>ICRU, "Neutron fluence, neutron spectra and kerma," International Commission on Radiation Units and Measurements, 1969 (unpublished).

<sup>13</sup>J. E. Turner, *Atoms, Radiation and Radiation Protection* (McGraw-Hill, New York, 1992).

<sup>14</sup>J. F. Ziegler, J. P. Biersack, and U. Littmark, *The Stopping and Range of Ions in Solids* (Pergamon, New York, 1985).

<sup>15</sup>A. B. Rosenfeld, G. I. Kaplan, M. G. Carolan, B. J. Allen, R. L. Maughan, M. Yudelev, C. Kota, and J. A. Coderre, "Simultaneous macro and micro dosimetry with MOSFETs," *IEEE Trans. Nucl. Sci.* **43**, 2693–2700 (1996).

<sup>16</sup>J. F. Briesmeister, "MCNP-4A General Monte Carlo Code for Neutron and Photon Transport," Los Alamos National Lab, LA-7396-M, Rev. 2, 1986 (unpublished).

<sup>17</sup>H. B. Liu, R. M. Brugger, D. D. Greenberg, D. C. Roger, J. P. Hu, and H. M. Hauptman, "Enhancement of the epithermal neutron-beam used for BNCT at BMRR," *Int. J. Radiat. Oncol., Biol., Phys.* **28**, 1149–1156 (1994).

<sup>18</sup>H. B. Liu, D. D. Greenberg, J. Capala, and F. J. Wheeler, "An improved neutron collimator for brain tumour irradiation in clinical BNCT," *Med. Phys.* **23**, 2051–2060 (1996).

<sup>19</sup>BNL, "Report BNL-325," Second Edition, 1958.